Spectroscopy and Predissociation of Acetylene in the np Gerade Rydberg States

Kazuhide Tsuji, Naoko Arakawa, Akio Kawai, and Kazuhiko Shibuya*

Department of Chemistry, Graduate School of Science and Engineering, Tokyo Institute of Technology, 2-12-1 Ohokayama, Meguro-ku, Tokyo 152-8551, Japan

Received: July 16, 2001; In Final Form: November 19, 2001

The *n*p gerade Rydberg states of acetylene were studied with various spectroscopic techniques to measure one-color resonant multiphoton ionization (REMPI) spectra, two-color REMPI mass spectra, fluorescence spectra, and fluorescence excitation spectra in the two-photon energy region of 72 000−92 000 cm^{-1}. The rotational analysis was successfully performed for one of the upper levels, which was assigned to the 4p $^1\Delta_g$ Rydberg state. All of the gerade Rydberg states prepared under the two-photon resonance conditions were found to be predissociative, and the two-photon preparation was accompanied by the fluorescence of the C_2 d $^3\Pi_g \rightarrow$ a $^3\Pi_u$ Swan system. In the fluorescence excitation spectra measured by monitoring the C_2 Swan system, higher members of the *n*p $^1\Sigma_g^+$ and $^1\Delta_g$ Rydberg series ($n \geq 4$) were observed and assigned for the first time. The predissociative lifetimes of the *n*p gerade Rydberg states are estimated from the spectral bandwidths. The mechanisms of the predissociation of acetylene in the Rydberg states and the formation of C_2 in the d $^3\Pi_g$ state are discussed.

Introduction

The electronic states of the molecules having a centrosymmetry are classified into gerade and ungerade species. Because of the rigorous selection rule of interaction, the excited-state dynamics of the gerade states may be different from that of the ungerade states. One good example of this kind of polyatomic molecule is acetylene in the Rydberg states. The ungerade Rydberg states of acetylene have been studied by using absorption,[1,2] resonance multiphoton ionization (REMPI),[3−8] and photofragment excitation[9,10] methods. Much information has been accumulated for the *n*s and *n*d ungerade Rydberg states and their lifetimes vary from tens of femtoseconds to more than 1 ps. However, information on the gerade Rydberg states is quite limited. Only the 3p gerade Rydberg states have been studied in detail spectroscopically. The 3p gerade Rydberg states were studied by (2+1) REMPI,[11] two-color double resonance spectroscopy via the $\tilde{A}$ ^1A_u state,[12] or fluorescence excitation spectroscopy.[13] Shafizadeh et al.[8] carried out the REMPI experiments of C_2H_2 but could not observe the *n*p gerade Rydberg states with $n \geq 4$. They mentioned the short lifetimes of the *n*p ($n \geq 4$) gerade Rydberg states as the reason that these states were not detected in the REMPI spectra. At this moment, it is not clear even whether they are predissociative or not, for lack of the spectroscopic information on the gerade Rydberg states. The spectroscopic study of the gerade Rydberg states is indispensable to understanding of the difference in the excited-state dynamics between the ungerade and gerade Rydberg states of acetylene.

In this work, we measured the excitation spectra due to the two-photon transition to the gerade Rydberg states of C_2H_2 by monitoring photofragment fluorescence (C_2 d $^3\Pi_g \rightarrow$ a $^3\Pi_u$ Swan band) or photoionized ion signals ($C_2H_2^+$, C_2^+). The C_2 Swan band was observed as in many other experiments of the UV photolysis of hydrocarbons with intense laser pulses.[14−16] Higher members of the *n*p $^1\Sigma_g^+$ and $^1\Delta_g$ Rydberg series ($n \geq 4$) were observed and assigned for the first time. The mechanisms for the predissociation of C_2H_2 in the gerade Rydberg states and the C_2 formation are discussed.

Experimental Section

REMPI spectra, time-of-flight (TOF) mass spectra, fluorescence excitation spectra, and fluorescence spectra were measured under the jet-cooled conditions. REMPI spectra were also measured at room temperature. The TOF mass spectrometer used in this study has been described in detail previously.[17] To measure one-color REMPI spectra and one-color TOF mass spectra, the output from a dye laser (Lumonics, HD-300) pumped by a third harmonic of a Nd:YAG laser (Lumonics, HY750) was frequency-doubled in a BBO crystal. Two-color REMPI experiments were performed with two dye lasers (Lumonics, HD-300) pumped by the third harmonics of a Nd:YAG laser (Lumonics, HY750). Both ν_1 and ν_2 laser beams were dye laser outputs frequency-doubled with a BBO or KDP crystal. The resultant ions were detected by a microchannel plate (MCP, Galileo Electro-Optics). To obtain TOF mass spectra, the output signals from the MCP detector were measured by a digital oscilloscope (Tektronics, TDS-620) and averaged over 1000 or 10 000 laser shots.

The fluorescence spectra were measured after jet-cooled acetylene was excited to a certain vibronic level observed in the REMPI spectra. The fluorescence was resolved by a grating monochromator (Nikon, G-500) and the transmitted radiation was monitored by a photomultiplier (Hamamatsu, R-928). The output signal was amplified by a current amplifier (Keithley, 427) and averaged by a gated integrator (Stanford Research, SR-250). Monitoring the emission light selected by optical filters (Toshiba, UV-29 and Y-44), we measured the fluorescence excitation spectra of acetylene. Calibration of laser wavelengths was accomplished by recording the optogalvanic spectra of Ne. Typical laser intensity used in the one-color experiments was 100 μJ/pulse.

* To whom correspondence should be addressed. E-mail: kshibuya@chem.titech.ac.jp. Fax: +81-0-5734-2655.

10.1021/jp015508i CCC: $22.00
Published on Web 01/12/2002

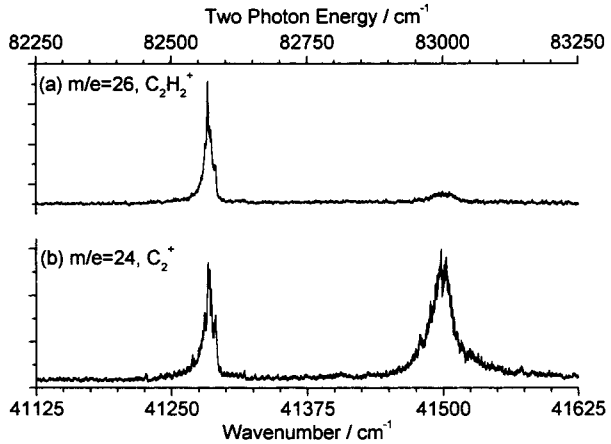

Figure 1. REMPI spectra of jet-cooled acetylene. The *m*/*e* values monitored are (a) 26 and (b) 24, corresponding to $C_2H_2^+$ and C_2^+, respectively.

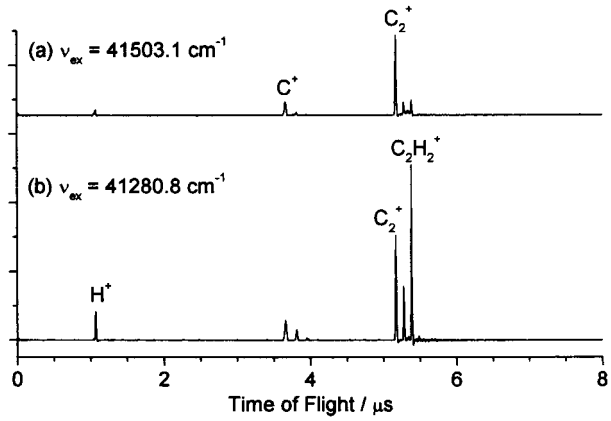

Figure 2. REMPI mass spectra of jet-cooled acetylene. The laser wavelengths are (a) 240.946 and (b) 242.244 nm corresponding to 83 006.1 and 82 561.5 cm^{-1}, respectively, in the two-photon energy.

Neat C_2H_2 was used without purification for jet-cooled experiments. C_2D_2 was synthesized by the reaction of CaC_2 with D_2O in a vacuum line.

Results and Discussion

REMPI Spectra and 4p Gerade Rydberg States. Figure 1 shows the REMPI spectra of jet-cooled acetylene measured by monitoring (a) $C_2H_2^+$ and (b) C_2^+. Two new bands were observed; one at the two-photon energy of 82 562 cm^{-1} is structured, and the other at 83 006 cm^{-1} is broad. It is found that the relative intensity of these two bands depends strongly on the mass number monitored. The intensity of the broad 83 006 cm^{-1} band is comparable to that of the structured 82 562 cm^{-1} band in the REMPI spectrum obtained by monitoring C_2^+, while the 83 006 cm^{-1} band is much weaker than the 82 562 cm^{-1} band in the $C_2H_2^+$-monitored REMPI spectrum. The TOF mass spectra measured at the two-photon energies of 83 006.1 and 82 561.5 cm^{-1} are shown as panels a and b, respectively, in Figure 2. The signals of C_2^+ and $C_2H_2^+$ are dominant in the TOF mass spectra measured at the two-photon energies of 83 006.1 and 82 561.5 cm^{-1}, respectively, which is consistent with the relative intensities of the two bands in the REMPI spectra of Figure 1. Many bands were also observed in the two-photon energy region below 82 250 cm^{-1}, which was almost the same result as Ashfold et al.[11] reported. No bands were observed in the two-photon energy region of 83 250−92 000 cm^{-1}, although we tried to measure the REMPI spectra.

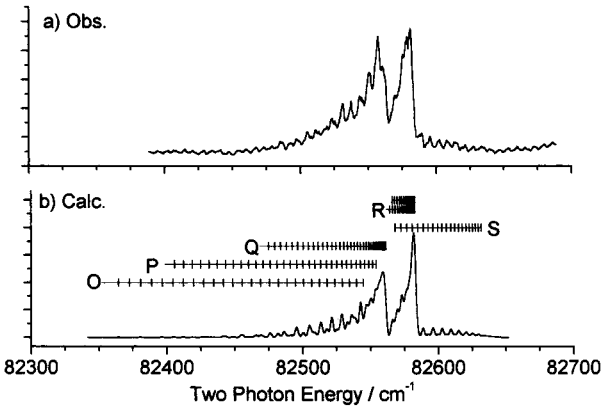

Figure 3. An expanded view of a structured band observed in the REMPI spectrum of acetylene at room temperature. Partially resolved rotational structure of the observed spectrum (a) is well reproduced by the spectrum (b) simulated assuming the two-photon $\Delta-\Sigma$ transition, the linewidth of 2.5 cm^{-1}, and the rotational temperature of 300 K.

The rotational structure of the 82 561 cm^{-1} band was partially resolved in the present experiment, and its overall band contour was successfully reproduced by the simulation of the rotational intensity calculation. The equation of two-photon absorption intensity of diatomic molecules was employed for the simulation.[18] Figure 3 shows the observed and calculated spectra of C_2H_2 measured at room temperature. The simulation was performed on the assumption that the rotational constants of C_2H_2 in the excited and ground states[19] are 1.115 and 1.176 608 cm^{-1}, respectively, and the vibronic symmetry of the excited state is Δ. The observed structure is well reproduced by the simulation as shown in Figure 3. The rotational structure of the same band measured under the jet-cooled conditions is also reproduced by the simulation employing the same values of parameters except for the rotational temperature. The rotational constants of $C_2H_2^+$ in the ground state[20] and C_2H_2 in the Rydberg states[2] are essentially the same as reported to be 1.104 and ~1.1 cm^{-1}, respectively. The rotational constant of the upper state responsible for this 82 561 cm^{-1} band (1.115 cm^{-1}) is also very close to those values. We also observed the similar structured and broad bands in the REMPI spectra of C_2D_2 in the same energy region. Isotope shifts for these two bands were very small at tens per centimeter, which indicates that both bands are due to the vibronic transitions between the zero-vibrational levels in the upper and lower electronic states. Because the three-photon energy is higher than the ionization potential[8] of acetylene (91 956 cm^{-1}), we conclude that $C_2H_2^+$ is formed by the (2+1) REMPI of C_2H_2 in this experiment.

Regarding the 3p gerade Rydberg states, the $^1\Delta_g$ and $^1\Sigma_g^+$ states have been observed in the (2+1) REMPI experiments.[11] The outer $1\pi_u$ orbital of acetylene in the ground state has atomic p character,[2] and the propensity rule for the two-photon absorption, $\Delta l = 0, \pm 2$, allows the excitation to the *n*p or *n*f Rydberg orbitals. Considering the rotational constant, isotope shifts, and the propensity rule for the two-photon transition, we assign the structured 82 561.5 cm^{-1} band to the 0−0 transition of C_2H_2 from $\tilde{X}^1\Sigma_g^+$ to a Rydberg state of $^1\Delta_g$ electronic symmetry. We have found that the upper state of the broad 83 006 cm^{-1} band is the zero-vibrational level of some electronic state, and it is tentatively assigned to the $^1\Sigma_g^+$ Rydberg state of C_2H_2 for the following reason. If the excited states observed in the present REMPI study are the 4p gerade Rydberg states of C_2H_2, the quantum defects (δs) are estimated to be 0.58 and 0.51 for the $^1\Delta_g$ and $^1\Sigma_g^+$ states, respectively. These values are in accord with the corresponding values for the 3p gerade

Rydberg states ($\delta = 0.61$ for $^1\Delta_g$ and $\delta = 0.51$ for $^1\Sigma_g^+$).[11] At this point, the structured 82 561 cm^{-1} and broad 83 006 cm^{-1} bands are assigned to the transitions to the 4p $^1\Delta_g$ and 4p $^1\Sigma_g^+$ Rydberg states, respectively. We will continue to discuss these assignments later.

Fragmentation Patterns Observed in TOF Mass Spectra. It is interesting to note that quite different fragmentation patterns were observed in the TOF mass spectra obtained by REMPI via two Rydberg states of C_2H_2, lying only 445 cm^{-1} apart. The fragmentation pattern via 4p $^1\Delta_g$ is almost the same as those via the 3p Rydberg states reported by Ashfold et al.,[11] in which $C_2H_2^+$ and C_2^+ ions are dominant in the TOF mass spectra. Some fraction of the fragment ion might be formed due to the photodissociation of parent $C_2H_2^+$ ion.[21] On the other hand, the parent $C_2H_2^+$ ion becomes minor and only C_2^+ remains dominant in the TOF mass spectrum obtained by REMPI via the 4p $^1\Sigma_g^+$ located at 445 cm^{-1} above the 4p $^1\Delta_g$ (Figure 2a). Furthermore, no REMPI signals were observed in the energy region above the location of 4p $^1\Sigma_g^+$. These observations suggest that 4p $^1\Sigma_g^+$ lying 83 006 cm^{-1} above the ground state of C_2H_2 may be located at a turning point in the fragmentation processes of the present interest, and the reason that only C_2^+ is dominant in the TOF mass spectrum via 4p $^1\Sigma_g^+$ is likely to provide information to understand why the *n*p Rydberg states with $n > 4$ were not observed in the REMPI spectrum.

We measured the laser power dependence of the $C_2H_2^+$ and C_2^+ ion yields via 4p $^1\Delta_g$. The resultant indexes of the power dependence are 1.8 for $C_2H_2^+$ and 3.1 for C_2^+. We also measured the laser power dependence of the C_2^+ ion yield via 4p $^1\Sigma_g^+$, and the resultant index is the same as that via 4p $^1\Delta_g$. In the lowest laser power limit, the index of laser power dependence will indicate the photon number to form the ions from the neutral parent molecule. At least three photons are required energetically for the ionization of C_2H_2, and therefore the measured index of 1.8 indicates the saturation in absorption under the present experimental conditions of REMPI. The formation of C_2^+ obviously required more photons (at least five photons). Candidate formation mechanisms of C_2^+ are as follows:

(i) Parent $C_2H_2^+$ ion generated by (2+1) REMPI can absorb further photons to form the ionic fragments. Photofragmentation yields of C_2^+ from $C_2H_2^+$ may strongly depend on the wavelengths. Possibly, the C_2^+ yield with the photolysis at 240.946 nm may be greatly larger than that at 242.244 nm.

(ii) Neutral acetylene, C_2H_2, in the 4p Rydberg states predissociates to form C2H and possibly C_2. The predissociation process competes with the photoionization process, which might be the case for the 4p $^1\Delta_g$ excitation. Upon the 4p $^1\Sigma_g^+$ excitation, the $C_2H_2^+$ ion signal might disappear because the predissociation of C_2H_2 4p $^1\Sigma_g^+$ dominates the photoionization. Photodissociation products of C2H and C_2 absorb further photons to form C_2^+.

The structured feature of the 82 561 cm^{-1} band means longer lifetime in 4p $^1\Delta_g$. The $C_2H_2^+$ ion signal is comparable with that of C_2^+ in the TOF mass spectrum obtained by REMPI via 4p $^1\Delta_g$. The broad feature of the 83 006 cm^{-1} band corresponding to the 4p $^1\Sigma_g^+ - \tilde{X}^1\Sigma_g^+$ transition implies the short lifetime in 4p $^1\Sigma_g^+$. The $C_2H_2^+$ ion signal drops in the TOF mass spectrum obtained by REMPI via 4p $^1\Sigma_g^+$. These observations support mechanism ii. To estimate the contribution of the photofragmentation of $C_2H_2^+$ to C_2^+ by mechanism i, we performed two-color TOF mass spectroscopic experiments described below.

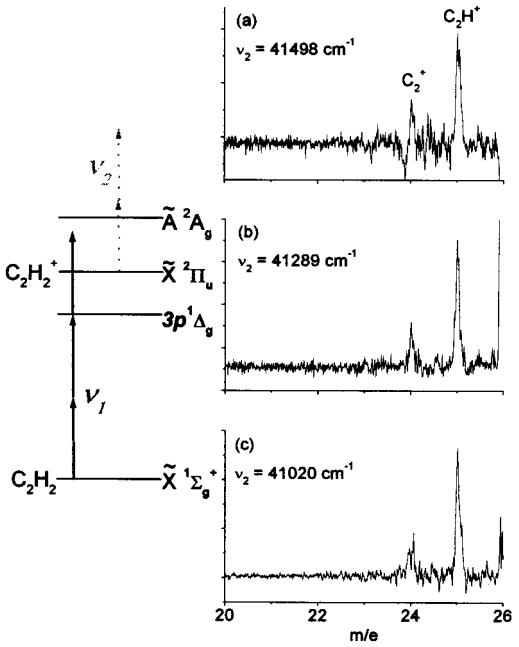

Figure 4. Two-color REMPI difference mass spectra of acetylene. The common ionization laser emitted at $2\nu_1 = 72\,744$ cm^{-1} in all of the spectra. The ν_2 wavenumbers correspond to (a) the two-photon 4p $^1\Sigma_g^+ \rightarrow \tilde{X}\ ^1\Sigma_g^+$ transition of C_2H_2, (b) the two-photon 4p $^1\Delta_g - \tilde{X}^1\Sigma_g^+$ transition of C_2H_2, and (c) the one-photon $\tilde{A}^2A_g$ (4^3)$-\tilde{X}^2\Pi_u$ transition of $C_2H_2^+$. In these experiments, to measure weak fragment ion signals precisely, we did not care the current saturation of the detector induced by the strong ion signal of parent ion.

The first ν_1 laser was used for the (2+1) three-photon absorption of acetylene to form $C_2H_2^+$. The ν_1 wavelength was chosen at 274.94 nm to minimize the ionic fragmentation. We employed the 3p $^1\Delta_g$ state as the intermediate for the (2+1) REMPI. Although C_2H^+ is known to be formed by the (1+1) photodissociation process via the ionic $\tilde{A}\ ^2A_g$ state, the one-photon energy of ν_1 (36 372 cm^{-1}) is lower than the $\tilde{A}^2A_g - \tilde{X}^2\Pi_u$ transition energy of $C_2H_2^+$ ($\geq$39 159 cm^{-1}).[21] The second ν_2 laser was used as a photolysis laser of $C_2H_2^+$. The flux of the ν_2 laser was adjusted to minimize the multiphoton ionization of C_2H_2. A variety of ν_2 wavenumbers were tested in the region of 41 020−41 666 cm^{-1} with the help of the reported spectrum [21] of the $C_2H_2^+$ $\tilde{A}^2A_g - \tilde{X}^2\Pi_u$. Under ideal experimental conditions, only $C_2H_2^+$ should be observed in the TOF mass spectrum ionized by ν_1 alone [spectrum (ν_1)], no ions should be observed in the TOF mass spectrum measured by ν_2 alone [spectrum (ν_2)], and the ionic fragments should be observed in the TOF mass spectrum measured by the simultaneous use of the ν_1 and ν_2 lasers [spectrum (ν_1 & ν_2)]. In the actual experiments, we could not avoid small contributions of the ν_1 and ν_2 lasers to ionic fragmentation and ionization, respectively. To eliminate these contributions and to extract information on the ionic fragmentation by the ν_2 laser, the difference spectra are obtained by the following treatment of spectra:

$$\text{difference spectrum} = \text{spectrum}\ (\nu_1\ \&\ \nu_2) - \text{spectrum}\ (\nu_1) - \text{spectrum}\ (\nu_2)$$

The lasers used are written in parentheses. Typical examples of these difference spectra are shown in Figure 4. The ν_2 wavenumbers correspond to (a) the two-photon 4p $^1\Sigma_g^+ - \tilde{X}^1\Sigma_g^+$ transition of C_2H_2, (b) the two-photon 4p $^1\Delta_g - \tilde{X}^1\Sigma_g^+$ transition of C_2H_2, and (c) the one-photon $\tilde{A}^2A_g$ (ν_4^3)$-\tilde{X}^2\Pi_u$ transition of $C_2H_2^+$.

The fragmentation patterns appearing in the TOF mass spectra at different ν_2 wavenumbers are essentially composed of strong C_2H^+ and weak C_2^+ signals as shown by spectra a, b, and c and more importantly do not change among spectra a, b, and c. We measured the difference TOF mass spectra at other ν_2 wavenumbers, but all of the patterns are similar. These observations indicate that the ionic photofragmentation process is wavenumber-independent in the energy region of 41 000−41 700 cm^{-1}. Thus, we conclude that the dominant source of C_2^+ is not the ionic photofragmentation due to mechanism i but is the neutral predissociation due to mechanism ii.

It should be mentioned here that one cannot exclude the possible involvement of the superexcited state of C_2H_2 (C_2H_2**) in addition to mechanism ii mentioned above. Energetically, it is possible to generate C_2H_2** by three-photon excitation of C_2H_2. Actually C_2H_2** has been studied by the VUV excitation in the spectral region above the ionization potential[8] (91 956 cm^{-1}), and the electronically excited C_2 product was observed.[22] The C_2 formation through the superexcited state might be one candidate to generate C_2^+, although the three-photon absorption of C_2H_2 via the short-lived 4p $^1\Sigma_g^+$ state (τ = 0.14 ps as discussed later) is likely to be very inefficient and less plausible.

Fluorescence Spectra of C_2 Photofragment. In our REMPI experiments, we have succeeded in observing the 4p gerade Rydberg states, while higher members of gerade Rydberg states have not been observed yet. The fragmentation patterns appearing in the TOF mass spectra imply the predissociation at the gerade Rydberg states of C_2H_2. Monitoring the predissociation products of parent molecule is a powerful method to probe the predissociative excited states in general, and we tried to measure the fluorescence of fragments formed by the multiphoton absorption via Rydberg states of C_2H_2.

The UV photofragmentation of neutral acetylene using 266 nm laser pulses was studied by Craig et al.[15] In the fluorescence spectrum following the photolysis of acetylene, they found that the dominant component of emission was a C_2 d $^3\Pi_g \rightarrow$ a $^3\Pi_u$ Swan system. We measured the fluorescence spectra of jet-cooled acetylene following the irradiation at 37 140, 41 281, and 41 503 cm^{-1} corresponding to the two-photon resonant (a) 3p $^1\Sigma_g^+-\tilde{X}^1\Sigma_g^+$, (b) 4p $^1\Delta_g-\tilde{X}^1\Sigma_g^+$, and (c) 4p $^1\Sigma_g^+-\tilde{X}^1\Sigma_g^+$ transitions, respectively. Figure 5 shows the observed fluorescence spectra, together with the Franck−Condon factors of the C_2 d $^3\Pi_g \rightarrow$ a $^3\Pi_u$ Swan system (d).[31] Apparently, the C_2 d $^3\Pi_g \rightarrow$ a $^3\Pi_u$ Swan system is the dominant component in all of the fluorescence spectra a−c, which is consistent with the results of the 266 and 193 nm multiphoton fragmentation studies reported previously.[15,16] Hsu et al. measured the dispersed fluorescence spectra upon multiphoton excitation of acetylene via the 3p $^1\Sigma_g^+$ state,[13] and they also observed the C_2 d $^3\Pi_g \rightarrow$ a $^3\Pi_u$ Swan system in the visible region.

The fluorescence spectra measured in this work are found to slightly depend on the excitation wavelength, though they are similar as shown in Figure 5. The shape and number of the peaks observed in the fluorescence spectrum are mainly governed by the vibrational state distribution of the photofragment C_2 d $^3\Pi_g$. Judging from the bandwidth of the $\Delta v = 0$ and +1 sequence bands observed at 500 and 460 nm, respectively, the vibrational state distribution for the photolysis via the 3p $^1\Sigma_g^+$ state is narrower than the distributions via the 4p $^1\Delta_g$ and $^1\Sigma_g^+$ states. In the fluorescence spectrum via the 3p $^1\Sigma_g^+$ state (Figure 5a), only $\Delta v = 0$ and +1 sequence bands are observed, but the $\Delta v = 2$ sequence band is not. This indicates that the photofragment C_2 d $^3\Pi_g$ is dominantly populated in the vibrational levels of $v = 0$ and 1.

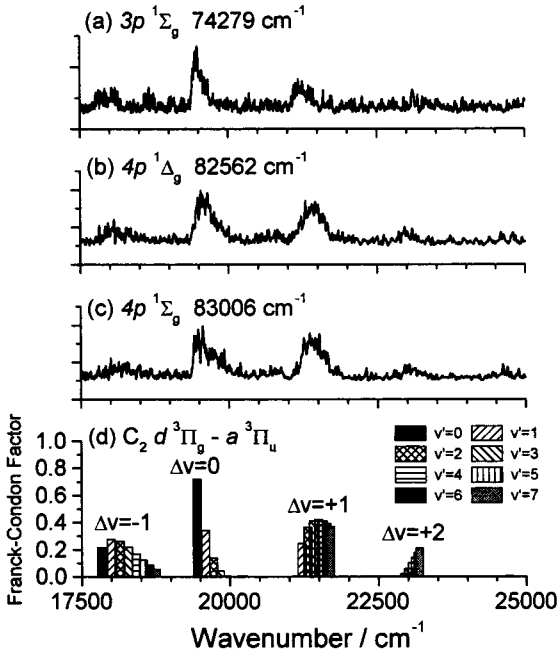

Figure 5. Fluorescence spectra of jet-cooled acetylene measured upon the two-photon excitations at (a) 74 279, (b) 82 502, and 83 006 cm^{-1}, which correspond to 3p $^1\Sigma_g^+-\tilde{X}^1\Sigma_g^+$, 4p $^1\Delta_g-\tilde{X}^1\Sigma_g^+$, and 4p $^1\Sigma_g^+-\tilde{X}^1\Sigma_g^+$ transitions, respectively. Franck−Condon factors are shown in panel d for the C_2 d $^3\Pi_g \rightarrow$ a $^3\Pi_u$ Swan system.

Fluorescence Excitation Spectra. The C_2 fluorescence observed in the multiphoton excitation of C_2H_2 via the gerade Rydberg states was used for probing these Rydberg states. We measured the fluorescence excitation spectra of jet-cooled C_2H_2 by monitoring the visible light in the 450−650 nm region under the conditions that the laser beam was tightly focused. This wavelength range covers the whole fluorescence of C_2 d $^3\Pi_g \rightarrow$ a $^3\Pi_u$. Figure 6 shows the overall fluorescence excitation spectrum measured. The observed peaks are classified into the following four groups.

Group i. A group of peaks, which have broad line widths, observed in the lower energy region of 36 000−39 500 cm^{-1} are due to the two-photon transitions to the gerade Rydberg states in the 72 000−79 000 cm^{-1} region assigned by Ashfold et al.[11] in their REMPI experiments and also reported by Hsu et al. in their LIF experiments.[13]

Group ii. A pair of broad and structured peaks observed at 82 562 and 83 006 cm^{-1} in the two-photon energy, respectively, are also recognized in the REMPI spectra in this work and are tentatively assigned to the two-photon transitions to the 4p gerade Rydberg states. These two bands are reported for the first time.

Group iii. A group of broad peaks observed in the higher energy region of 41 500−44 500 cm^{-1} were also observed for the first time.

Group iv. A group of structured peaks observed in the higher energy region of 41 500−46 000 cm^{-1} are due to the one-photon transition to the vibrational levels in the $\tilde{A}$ ^1A_u state, most of which have been already reported.[19,23] These bands were also observed in the fluorescence excitation spectra measured under the unfocused laser beam conditions. We detected C_2H_2 $\tilde{A}$ $^1A_u \rightarrow \tilde{X}$ $^1\Sigma_g^+$ fluorescence because the photon energies are less than the C−H bond dissociation energy[24] of 46 074 cm^{-1} and the ultraviolet $\tilde{A}$ $^1A_u \rightarrow \tilde{X}$ $^1\Sigma_g^+$ fluorescence extends to the visible region.[25−27]

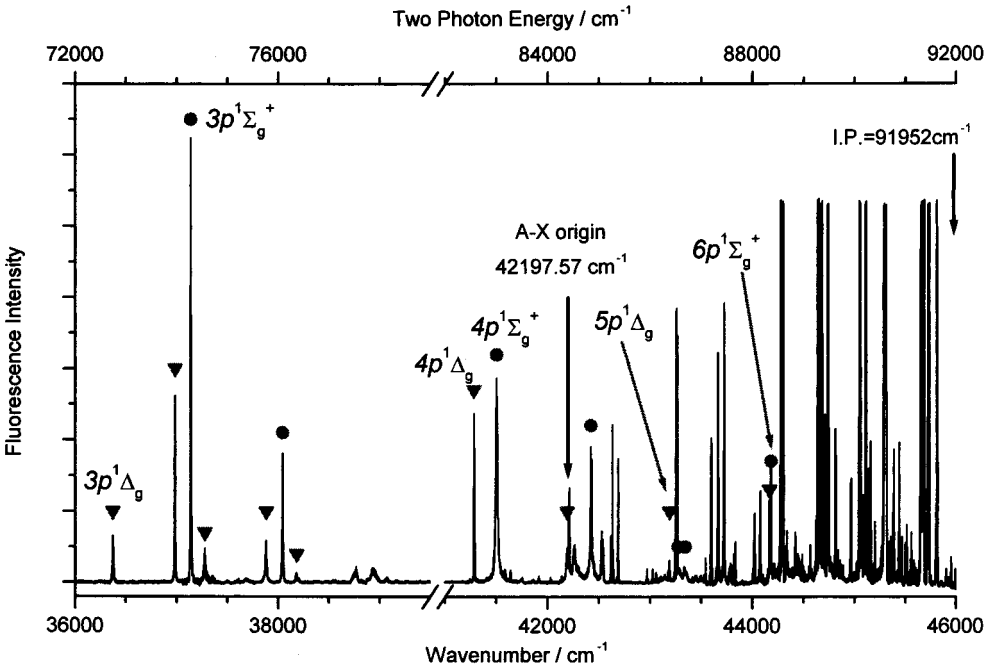

Figure 6. Two-photon fluorescence excitation spectrum of jet-cooled acetylene obtained by monitoring the whole fluorescence of C_2 d $^3\Pi_g \rightarrow$ a $^3\Pi_u$ Swan system. The members of the Rydberg series of C_2H_2 are indicated by the symbols of the circle and the triangle. The one-photon $\tilde{A}^1A_u-\tilde{X}^1\Sigma_g^+$ transition peaks also appear above the $\tilde{A}^1A_u-\tilde{X}^1\Sigma_g^+$ origin at 42 198 cm^{-1}.

TABLE 1: Peak Position, Assignment, Quantum Defect, Widths, and Lifetime of the C_2H_2 Bands Observed in the Fluorescence Excitation Spectrum

peak position[a] (cm^{-1})	fwhm (cm^{-1})	lifetime[b] (ps)	assignment	quantum defect[c]
72 744.1	22.0	0.24	3p $^1\Delta_g$ 0^0	0.61
73 969.3	11	0.47	3p $^1\Delta_g$ 4^2	
74 279.0	9.2	0.58	3p $^1\Sigma_g^+$ 0^0	0.51
74 554	~40	~0.1	3p $^1\Delta_g$ 2^1	
75 760.8	27	0.20	3p $^1\Delta_g$ 2^14^2	
76 085.0	15	0.35	3p $^1\Sigma_g^+$ 2^1	
76 360	~40	~0.1	3p $^1\Delta_g$ 2^2	
77 520	~100	~0.05		
77 880	~100	~0.05		
82 561.5	(2.5)[d]	(>2.1)	4p $^1\Delta_g$ 0^0	0.58
83 006	39	0.14	4p $^1\Sigma_g^+$ 0^0	0.50
84 380	~40	~0.1	4p $^1\Delta_g$ 2^1	
84 526	~40	~0.1		
84 845			4p $^1\Sigma_g^+$ 2^1	
85 060				
86 380	(~4)[d]	(~1)	5p $^1\Delta_g$ 0^0	0.56
86 550			5p $^1\Sigma_g^+$ 0^0	0.50
86 690			4p $^1\Sigma_g^+$ 2^2	
88 333	11	0.47	6p $^1\Delta_g$ 0^0	0.60
88 360	7.9	0.67	6p $^1\Sigma_g^+$ 0^0	0.50
89 675	~20	~0.3		

[a] Two-photon energy. Peaks belonging to group iv are not included. [b] The relation fwhm (cm^{-1}) = $5.3/\tau$ (ps) is applied. [c] Quantum defects are calculated from the relation E (cm^{-1}) = 91 956−109 737/$(n-\delta)^2$. [d] Determined by the rotational simulation (see text).

The positions of peaks classified into groups i, ii, and iii are listed in Table 1, together with the widths.

The bands belonging to group iii are likely due to the two-photon transitions to the gerade Rydberg states for the following reasons. First, these bands were not observed in the fluorescence excitation spectra measured under the unfocused laser beam conditions. Second, these bands have not been reported in the absorption spectra of acetylene in the 41 500−44 500 cm^{-1} region.[19,23] On the assumption that the upper levels of the two-photon transitions (group iii) are Rydberg states, we calculate the quantum defect (δ) using the appropriate principal quantum number (n) listed in Table 1. The propensity rule for the two-photon absorption, $\Delta l = 0, \pm 2$, allows the excitation to the np or nf Rydberg orbitals. Because the quantum defects (δs) for the nf Rydberg states are expected to be almost zero and the listed δ values are around 0.6, the upper Rydberg states seem to be of the np Rydberg series. Thus, we propose that the newly observed broad bands (Group iii) are due to the two-photon transitions to the np gerade Rydberg states of acetylene.

Two bands observed at 82 561.5 and 86 380 cm^{-1} show partially resolved rotational structures in the fluorescence excitation spectra. The observed structure of the 82 561 cm^{-1} band is well reproduced by the simulation as shown in Figure 7. The rotational structure of the same band measured by using the REMPI method is also reproduced by the simulation employing the same values of rotational constants (Figure 3). This band is assigned to the transition to the 4p $^1\Delta_g$ state. The 86 380 cm^{-1} band is also likely to be the $\Delta-\Sigma$-type transition, though it is broad and rather difficult to be compared with the simulation. The quantum defect of this upper state, calculated to be 0.56 on the assumption that the principal quantum number is 5, is almost the same value as those of the 3p $^1\Delta_g$ and 4p $^1\Delta_g$ states. Thus, we assign the 86 380 cm^{-1} band to the transition to the 5p $^1\Delta_g$ state. Unfortunately, the other bands except for the 82 561.5 and 86 380 cm^{-1} bands observed in the fluorescence excitation spectra are diffuse and show no rotational structure.

Quantum Defect and Identification of *n*p Rydberg Series. In general, it is quite difficult to spectroscopically identify the upper levels of the diffuse bands, which show no rotational structure, because we have no way to determine the vibronic symmetry and rotational constants for these upper levels. Considering the quantum defects, vibrational frequencies, and band intensities, we tentatively assigned the diffuse bands to the transition to the np gerade Rydberg states as listed in Table 1. To confirm the assignments, the quantum defects are plotted

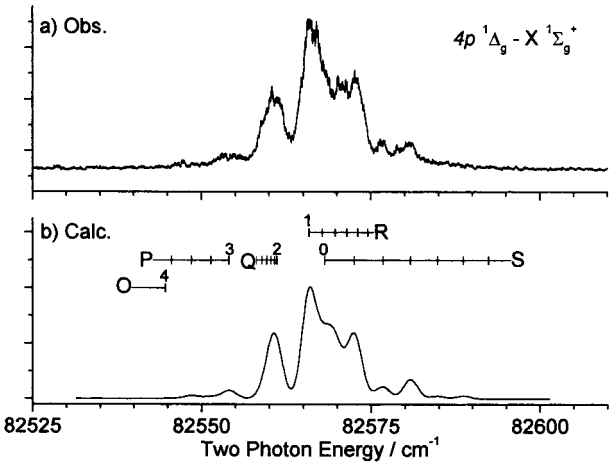

Figure 7. An expanded view of a structured band in the fluorescence excitation spectrum of jet-cooled acetylene obtained by monitoring the C_2 Swan band emission. Partially resolved rotational structure (a) is well reproduced by the simulation (b) assuming the two-photon $\Delta-\Sigma$ transition, the line width of 2.5 cm^{-1}, and the rotational temperature of 15 K. The band is assigned to 4p $^1\Delta_g \rightarrow \tilde{X}\ ^1\Sigma_g^+\ 0^0$.

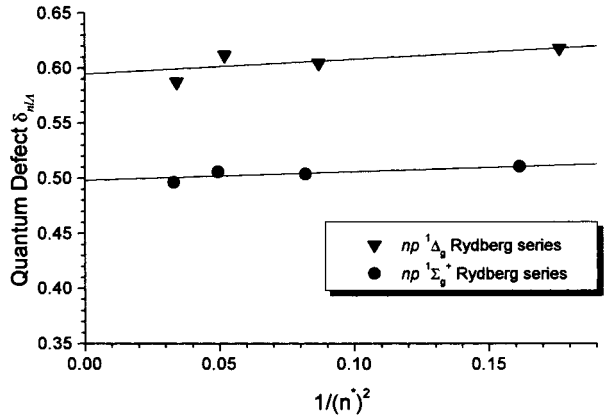

Figure 8. Edlèn plots of *n*p Rydberg series for acetylene.

according to the following Rydberg−Ritz equation[28] as shown in Figure 8.

$$\delta_{nl\Lambda} = \delta_0 + \frac{\delta_2}{(n-\delta_0)^2}$$

This equation describes the slight *n*-dependence of the quantum defect. Here, $\delta_{nl\Lambda}$ is the quantum defect for a Rydberg state with principal quantum number *n*, orbital angular momentum *l*, and electronic symmetry Λ. The symbols of δ_0 and δ_2 are the parameters. The horizontal axis represents the effective quantum number $n^* = (n - \delta_0)$. The quantum defects ($\delta_{nl\Lambda}$'s) are well reproduced by this simple equation, and we obtain the convergence limits of 92 078 and 91 983 cm^{-1} for the *n*p $^1\Delta_g$ and *n*p $^1\Sigma_g^+$ Rydberg series, respectively, which agree with the ionization potential[8] of acetylene (91 956 cm^{-1}). The δ_0 values are 0.59 ± 0.02 for the *n*p $^1\Delta_g$ Rydberg series and 0.50 ± 0.01 for the *n*p $^1\Sigma_g^+$. The δ_0 values are reported to be 0.976 for the *n*sσ_g $^1\Pi_u$ and 0.47 for the *n*dπ_g $^1\Sigma_u^+$.[2] The δ_0 values (0.59 and 0.50) for the newly observed Rydberg states are a bit larger than 0.47 for *n*d and smaller than 0.976 for *n*s. Judging from this quantum defect analysis, we are confident that all of the upper levels shown in Figure 8 belong to the *n*p Rydberg series ($n = 3-6$) and the proposed assignments listed in Table 1 are correct.

Formation of C_2 d $^3\Pi_g$. In the fluorescence excitation spectrum shown in Figure 6, there are many peaks due to the two-photon transition to the *n*p Rydberg states. Especially, the 5p and 6p Rydberg states were observed for the first time in the fluorescence excitation spectrum. The observed fluorescence is considered to be the C_2 d $^3\Pi_g \rightarrow$ a $^3\Pi_u$ Swan system as in the cases of 3p $^1\Sigma_g^+$ and 4p Rydberg states. Two plausible formation mechanisms of C_2 d $^3\Pi_g$ are considered below. One is the predissociation of C_2H_2 in the gerade Rydberg states to C_2H, followed by the further photodissociation of C_2H to form C_2 d $^3\Pi_g$. As described before, the width of the 4p $^1\Sigma_g^+ - \tilde{X}^1\Sigma_g^+$ transition (83 006 cm^{-1} band) corresponds to a lifetime of 0.14 ps, which implies that the predissociation dominates the photoionization of C_2H_2 in the 4p $^1\Sigma_g^+$ state. Hsu et al. reported that the most C_2 d $^3\Pi_g$ are formed by this predissociation mechanism when acetylene was excited by multiple photons via 3p $^1\Sigma_g^+$ state.[13] Another mechanism is the dissociation of C_2H_2 in the superexcited states to C_2 d $^3\Pi_g$.[22,29,30] Three photons of an energy that, at the two-photon energy, would populate the 3p and 4p gerade Rydberg states would reach the 108 000−126 000 cm^{-1} region. Ukai et al.[22] observed the C_2 d $^3\Pi_g \rightarrow$ a $^3\Pi_u$ Swan band following photoirradiation in the extreme UV region (105 000−154 000 cm^{-1}). They found that the photodissociation of C_2H_2 in the superexcited states to form C_2 d $^3\Pi_g$ competes with the ionization process and the photodissociation quantum yield is nearly constant over the spectral region. If the C_2 d $^3\Pi_g$ product observed in the present study is also formed via the superexcited states of C_2H_2, the fluorescence excitation spectrum (Figure 6) should be similar to the $C_2H_2^+$-monitored REMPI spectrum (Figure 1a). However, the relative intensity of the 83 000 cm^{-1} band to the 82 570 cm^{-1} band in the fluorescence excitation spectrum (Figure 6) is quite different from that in the $C_2H_2^+$-monitored REMPI spectrum (Figure 1a). This consideration also supports the first mechanism that C_2 d $^3\Pi_g$ is formed through the predissociation of the *n*p gerade Rydberg states of C_2H_2.

Predissociation of Rydberg States. The photodissociation of C_2H_2 in the ungerade Rydberg states has been studied by Löffler et al.[10] Especially, the 2^1 level of the $\tilde{H}$ $^1\Pi_u$ Rydberg state lying at 82 260 cm^{-1} is well investigated by the measurement of the kinetic energy distribution of H atoms. The internal energy distribution of the counter C_2H product consists of two components; one is broad and smooth, and another is structured because of the vibrational excitation of $C_2H(\tilde{A}\ ^2\Pi)$. The broad and smooth component extends to the maximum limit of the available energy of C_2H and presents a peak at a relatively high internal energy. The distribution is well reproduced by the phase-space theory, and then, the following predissociation mechanism is proposed: C_2H_2 ($\tilde{H}$ $^1\Pi_u$) → $C_2H_2(\tilde{A}\ ^1A_u) \rightarrow C_2H + H$.

If the predissociation of C_2H_2 in the gerade Rydberg states of the present interest proceeds via predissociative valence excited states, the internal energy distribution of C_2H may be broad and extend to the maximum limit of the available energy. The C_2 d $^3\Pi_g$ fragment can be formed by the further photon absorption of such a hot C_2H fragment. The C_2 d $^3\Pi_g$ fragment formed by the multiphoton dissociation of C_2H_2 via the 3p $^1\Sigma_g^+$ state was found to be mainly populated in the vibrational levels of $v = 0$ and 1 as mentioned before. The maximum vibrational quantum number of C_2 d $^3\Pi_g$ by the three-photon absorption is calculated to be 3, which is consistent with the experimental result of the narrow vibrational distribution in C_2 d $^3\Pi_g$.

The lifetimes of the ungerade Rydberg states vary from 50 fs to more than 10 ps but do not show a simple trend. For example, the $\tilde{G}$ $^1\Pi_u$ ($T_0 = 80\,130$ cm^{-1}) and $\tilde{H}$ $^1\Pi_u$ ($T_0 = 80\,450$

cm^{-1}) states belong to the 3s + 4d supercomplex, but their lifetimes are quite different at >2 ps and 60 fs, respectively.[9] Such a fluctuation in the lifetimes of the ungerade Rydberg states indicates not the direct predissociation to a repulsive potential energy surface but the indirect predissociation mechanism via valence excited states.[10] The lifetimes of the gerade Rydberg states vary from 0.14 ps to more than 2 ps. It is found that the lifetimes of the gerade Rydberg states do not seem to depend on the principal quantum number, the vibrational quantum number, the symmetry of the Rydberg orbital, and so on. In short, they show no simple tendency as in the ungerade Rydberg states. This fluctuation in the lifetimes of the gerade Rydberg states implies that the gerade Rydberg states predissociate via the predissociative valence excited states. It is interesting to note that the intensities of the transitions to the *n*p Rydberg states in Figure 6 also exhibit the strong fluctuation.

As already mentioned in the Introduction, the reported REMPI studies have failed to find the *n*p gerade Rydberg series ($n \geq 4$). One explanation for that is based on the shortness of the lifetimes of the *n*p ($n \geq 4$) gerade Rydberg states. As shown in Table 1, their lifetimes are not always shorter than those of the 3p gerade Rydberg states, and the predissociation lifetimes of 3p and 6p gerade Rydberg states are almost the same. These facts seem to be incompatible with the past interpretation that no REMPI signals were observed for the *n*p ($n \geq 4$) gerade Rydberg states due to the predissociation. In the one-color (2+1) REMPI process, both the two-photon absorption rate to a Rydberg state and the photoionization rate from that state may become slower with increasing *n*. It remains, therefore, an unsettled problem why the bands to higher-*n* Rydberg states do not appear in the (2+1) REMPI spectra.

Summary

The *n*p gerade Rydberg states ($n = 4-6$) of acetylene were observed for the first time. The multiphoton process via these *n*p gerade Rydberg states results in the formation of C_2 in the d $^3\Pi_g$ state. The lifetimes of the *n*p gerade Rydberg states fluctuate randomly, which indicates that the photodissociation occurs via the predissociative valence excited states. It is demonstrated that the fluorescence excitation spectroscopy by monitoring the C_2 d $^3\Pi_g \rightarrow$ a $^3\Pi_u$ Swan system is powerful to study the predissociative excited states of acetylene and possibly other hydrocarbons.

References and Notes

(1) Herman, M.; Colin, R. *J. Mol. Spectrosc.* **1981**, *85*, 449.
(2) Herman, M.; Colin, R. *Phys.ica Scr.* **1982**, *25*, 275.
(3) Ashfold, M. N. R.; Dixon, R. N.; Prince, J. D.; Tutcher, B. *Mol. Phys.* **1985**, *56*, 1185.
(4) Ashfold, M. N. R.; Heryet, C. D.; Prince, J. D.; Tutcher, B. *Chem. Phys. Lett.* **1986**, *131*, 291.
(5) Zhu, Y. F.; Shehadeh, R.; Grant, E. R. *J. Chem. Phys.* **1993**, *99*, 5723.
(6) Orlando, T. M.; Anderson, S. L.; Appling, J. R.; White, M. G. *J. Chem. Phys.* **1987**, *87*, 852.
(7) Fillion, J. H.; Campos, A.; Pedersen, J.; Shafizadeh, N.; Gauyacq, D. *J. Chem. Phys.* **1996**, *105*, 22.
(8) Shafizadeh, N.; Fillion, J.-H.; Gauyacq, D.; Couris, S. *Philos. Trans. R. Soc. London, Ser. A* **1997**, *355*, 1637.
(9) Löffler, P.; Lacombe, D.; Ross, A.; Wrede, E.; Schnieder, L.; Welge, K. H. *Chem. Phys. Lett.* **1996**, *252*, 1996.
(10) Löffler, P.; Wrede, E.; Schnieder, L.; Halpern, J. B.; Jackson, W. M.; Welge, K. H. *J. Chem. Phys.* **1998**, *109*, 5231.
(11) Ashfold, M. N. R.; Tutcher, B.; Yang, B.; Jin, Z. K.; Anderson, S. L. *J. Chem. Phys.* **1987**, *87*, 5105.
(12) Takahashi, M.; Fujii, M.; Ito, M. *J. Chem. Phys.* **1992**, *96*, 6486.
(13) Hsu, Y.-C.; Lin, M.-S.; Hsu, C.-P. *J. Chem. Phys.* **1991**, *94*, 7832.
(14) Martin, M. *J. Photochem. Photobiol. A: Chem.* **1992**, *66*, 263.
(15) Craig, B. B.; Faust, W. L.; Goldberg, L. S.; Weiss, R. G. *J. Chem. Phys.* **1982**, *76*, 5014.
(16) Okabe, H.; Cody, R. J.; Allen, J. E., Jr. *Chem. Phys.* **1985**, *92*, 67.
(17) Tsuji, K.; Shibuya, K.; Obi, K. *J. Chem. Phys.* **1994**, *100*, 5441.
(18) Bray, R. G.; Hochstrasser, R. M. *Mol. Phys.* **1976**, *31*, 1199.
(19) Watson, J. K. G.; Herman, M., Van Craen, J. C.; Colin, R. *J. Mol. Spectrosc.* **1982**, *95*, 101.
(20) Jagod, M.-F.; Rösslein, M.; Gabrys, C. M.; Rehfuss, B. D.; Scappini, F.; Crofton, M. W.; Oka, T. *J. Chem. Phys.* **1992**, *97*, 7111.
(21) Cha, Ch.; Weinkauf, R.; Boesl, U. *J. Chem. Phys.* **1995**, *103*, 5224.
(22) Ukai, M.; Kameta, K.; Chiba, R.; Nagano, K.; Kouchi, N.; Shinsaka, K.; Hatano, Y.; Umemoto, H.; Ito, Y.; Tanaka, K. *J. Chem. Phys.* **1991**, *95*, 4142.
(23) Van Craen, J. C.; Herman, M.; Colin, R.; Watson, J. K. G. *J. Mol. Spectrosc.* **1985**, *111*, 185.
(24) Mordaunt, D. H.; Ashfold, M. N. R. *J. Chem. Phys.* **1994**, *101*, 2630.
(25) Yamanouchi, K.; Ikeda, N.; Tsuchiya, S.; Jonas, D. M.; Lundberg, J. K.; Adamson, G. W.; Field, R. W. *J. Chem. Phys.* **1991**, *95*, 6330.
(26) Solina, S. A. B.; O'Brien, J. P.; Field, R. W.; Polik, W. F. *J. Phys. Chem.* **1996**, *100*, 7797.
(27) Tsuji, K.; Terauchi, C.; Shibuya, K.; Tsuchiya, S. *Chem. Phys. Lett.* **1999**, *306*, 41.
(28) Gallagher, T. F. *Rydberg Atoms*; Cambridge University Press: Cambridge, U.K., 1994.
(29) Han, J. C.; Ye, C.; Suto, M.; Lee, L. C. *J. Chem. Phys.* **1989**, *90*, 4000.
(30) Hattori, H.; Hikosaka, Y.; Hikida, T.; Mitsuke, K. *J. Chem. Phys.* **1997**, *106*, 4902.
(31) Danylewych, L. L.; Nicholls, R. W. *Proc. R. Soc. London, Ser. A* **1974**, *339*, 197.